

Chapter 2

Fabrications of Side-Polished Fiber Components

2.1 Overview

Side-polishing technique had been developed for more than two decades. Variant kinds of fiber components such as gyros [1], couplers [2-5], splitters [6,7], delay-line [8,9], switches [10-12], filters [13-19], polarizers [20-23], modulators [24-26], attenuators [27], refractometers [28,29], amplifiers and lasers [30-35], sensors [36-42], etc., were fabricated by a side-polishing technique. In general, the side-polishing is to embed bare fibers into the grooves on silica or silicon substrates and the cladding is then partially polished away until the evanescent wave can be accessed. Subsequently, the polished fiber is characterized by liquid-drop tests to identify the polishing depth and length. The advantages of side-polished fiber devices are all-fiber, less polarization-sensitivity, no higher-order modes excitation, and so on. Unfortunately, in contrast to the fused-tapered fiber devices, the side-polished fibers are usually regarded time-consuming and expensive in fabrication. Moreover, the side-polished fiber devices are unstable to environment and difficult to control the uniformity. Hence, side-polished fiber components were not widely seen in commercial fiber-optic communication systems. However, side-polished fiber devices can still be a good candidate for investigating new physical phenomena when a new material or a material with a new structure is available. In this chapter, the fabrication of the side-polished fibers and their applications are discussed.

2.2 Side-Polished Single-Mode Fiber with a Long-Interaction Length

In this section, the procedures of fabricating and calibrating side-polished fibers using precision silicon V-grooves and liquid-drop test will be introduced, respectively. The polishing depth is controlled by the dimension of the etched V-groove while the interaction length is determined by the radius of curvature. The side-polished fiber with a larger radius of curvature and a central remaining cladding thickness of around 1 μm can have stronger evanescent wave interaction.

2.2.1 Fabrication

A side-polished fiber can be made by polishing the fiber with a motor-driven polishing wheel [43] or by embedding the bare fibers on a V-groove on silica [2, 44-46] or silicon substrate [8-9, 47-49] shown in Fig. 2.1 and polish the cladding above the silicon surface away. In contrast to silica substrate, side-polished fibers using a silicon substrate has the following advantages. First, the polishing depth and radius of curvature can be precisely controlled since the V-grooves on the silicon substrate are made by readily available microelectronic photolithography while the V-grooves on silica substrate are lathed mechanically. Accordingly, a side-polished fiber with a desired polishing depth and a uniform bending with large radius of curvature can be easily achieved. This is very important for polishing fiber with a gain medium or photonic crystal structure in which the liquid-drop test can not be used to calibrate the polishing depth [50]. Second, the fabrication is faster since the hardness of the silicon is much harder than that of silica. Thus, it normally takes around 30 minutes for us to finish side-polishing a fiber with radius of curvature of 800 cm, which is definitely a time-saving process around the world. Third, alignment V-grooves can be simultaneously made on a silicon substrate [47, 49] to solve the conventional difficulties in precision alignment for side-polished fiber components using silica substrate. Fourth, a larger radius of curvature of side-polished fibers can give rise to a longer effective interaction length which is beneficial to achieve a high extinction ratio of power and to make high efficiency devices using fiber grating [49], gain [51], or nonlinear mediums on the side-polished surface.

The fabrications of side-polished fibers are as follows. First, (100)-oriented silicon

wafers are deposited with silicon nitride with the thickness of around 1500 Å. Second, the V-groove patterns are then transferred to the photo-resist coated onto the silicon nitride by photolithography. The V-groove pattern is a line with its width gradually increases from center to the bilateral sides, which makes etched V-groove curved due to anisotropic etching. Third, the patterned silicon nitride is dry etched by plasma to define the positions for polished fibers. Fourth, the silicon wafers with open windows on silicon nitride are etched by KOH at 100°C for around eight hours to obtain the required width of the V-grooves shown in Fig. 2.2(a). Fifth, a section of fiber jacket is stripped and then embedded and glued into the V-groove using UV-curing epoxy. Sixth, the glued fibers are polished by a polisher with polishing slurry with the particle size of around 60 nm. The polishing process will be automatically stopped while the silicon wafer surface is touched, i.e. till to the polishing pad. Finally, the side-polished fiber is fulfilled shown in Fig. 2.2(b) and its characteristics of the side-polished fibers are calibrated by index-matching liquids and fitting the Leminger-Zengerle (L-Z) formula [52] as follows.

$$P_{liq} \cong P_{air} \cdot e^{-\alpha \cdot L_{eff}}$$



where P_{liq} and P_{air} are the output powers of the side-polished fiber in liquid and in air, respectively. α is power attenuation coefficient of the fundamental mode and L_{eff} is effective interaction length. α is expressed in terms of normalized parameters and is give by

$$\alpha = \frac{4\sqrt{2}}{a} \frac{1-b}{V} \sqrt{\Delta(1+2\Delta)} \frac{V_{ex}^2 - bV^2}{V_{ex}^2 K_1^2(V\sqrt{b})} \times \int_0^1 \sqrt{1-x^2} e^{-(2Vd/a) \left[\left(\frac{V_{ex}^2}{V^2} - b \right) x^2 + b \right]^{1/2}} dx; V_{ex} \geq b\sqrt{V}$$

where d is the distance from the polished fiber surface to the center of the fiber core.

K_1 , a , b , Δ , V , and V_{ex} are the modified Bessel function of the second kind of the first order, radius of the fiber core, normalized propagation constant of the fundamental mode, relative index difference between core and cladding, fiber V-value, and normalized external medium V-value, respectively. The last parameter is defined as

$$V_{ex} = \frac{2\pi a}{\lambda_0} \sqrt{n_{ex}^2 - n_{cl}^2}; n_{ex} \geq n_{cl}$$

where n_{ex} and n_{cl} are the refractive indices of the external medium and the fiber cladding, respectively.

2.2.2 Calibration and Measurement

For side-polished fibers, the remaining cladding thickness, radius of curvature, and effective interaction length are important parameters for side-polished fiber devices. They can be calibrated by liquid-drop tests in which index-matching liquids with different refractive indices are respectively applied on side-polished fibers to measure the corresponding output power. When the external medium is applied on side-polished fibers, the effective index of the side-polished fiber is perturbed and changed, shown in Fig. 2.3(a), by external medium through evanescent field. By doing so, the spectral responses of a side-polished single-mode fiber with radius of curvature of 1,500 cm at different indices of external medium are shown in Fig. 2.3(b). The extinction ratio of power at 1.55 μm can be higher than 90 dB and, through extrapolation using the L-Z formula, the effective interaction length is estimated to be about 16 mm which is much longer than that of using silica substrate [45]. The effective interaction length is proportional to the square root of radius of curvature [52] and thus a large radius of curvature can result in a longer effective interaction length.

2.3 Fused-Polished Fiber Coupler

Since the guiding area of the fused-tapered fiber coupler is in a dumbbell shape shown in Fig. 2.4, side-polished fiber coupler, in contrast, is polarization isotropic. It means that the polarization mode dispersion can be highly reduced and a narrowband fiber component is feasible. This is advantageous to make fiber components for the

high-bit-rate (above 40 Gb/s) fiber-optic communication systems. In addition, fused-polished fiber couplers can avoid the use of buffered index-matching liquids, which make the side-polished fiber coupler stable to the environment.

2.3.1 Introduction

Fiber couplers are essential components in fiber-optic communication systems. They normally serve as power dividers while those specially made can serve as narrow-band wavelength multiplexers. Two fabrication methods were demonstrated. The first method, proposed by Kawasaki *et al.* was to heat and then to pull two adjacent un-jacketed fibers together [53]. Accordingly, these couplers were named fused-tapered fiber couplers and had been mass-produced nowadays because of relative simplicity, in fabrication low cost, and reliability. The guiding-wave effect by the high-index core, however, of the tapered cores almost disappear in fused-tapered devices and this will affect the performance of certain all-fiber devices. One good example is the fused-type fiber-optic add/drop filters where Bragg gratings are formed in the elongated waist of the couplers [54]. Besides, the greatly asymmetrical cross-section of fused-tapered couplers will cause polarization degradation, thereby being problematic in achieving wavelength division multiplexing (WDM) components [54], particularly for those narrow-band devices. The second method is to use a side-polishing technique, depicted as follows [55]. Fibers are bonded into curved slots on quartz or glass substrate and are polished to access to fiber evanescent field. Later, two polished half-couplers are aligned and mated as a full-coupler. Unfortunately, both controlling a precise polishing depth and subsequent alignment were reported as time-consuming and tedious. In addition, the size is an issue. Both structures have their advantages and disadvantages. It is a very challenging question how to combine advantages of these two structures only. These stimulated us to propose a new structure here.

In early 1990s, Cryan *et al.* reported fused-polished couplers [56]. They polished fibers directly using an abrasive polishing wheel and then fused two polished fibers using a flame. Prior to fusion, a thin layer of silica deposited onto the fiber assembly

by sol-gel method was recommended. However, insertion losses, mechanical strength and a long interaction length of polished fibers turned out to be difficult. By contrast, we propose a new method of fabricating fused-polished fiber couplers using a home-made polisher and a home-made fusion station. The fabrication is presented next.

2.3.2 Experimental Results and Discussion

In this dissertation, Corning SMF-28 1.55- μm single-mode fibers are used. Silicon wafers are employed as our polishing substrates where multiple, precision curved V-grooves are made using standard microelectronic processing techniques. The unjacketed fibers are loaded and glued into these grooves, and then are polished them using a home-made polisher. Characterizations of polished fibers are proceeded using the liquid-drop tests [52]. An effective interaction length as long as about 12 mm at 1.55- μm [57] and their surface roughness, examined by atomic force microscopy (AFM), better than few tens of nanometers were also achieved and shown in Fig. 2.5.

The polished fibers on the wafer are sliced into several pieces and each piece contains a polished fiber. For each sample, the two leading ends of polished fiber are bilaterally loaded onto a specially designed mechanical mount, equipped with a micrometer at one side, with polished surface oriented and fixed. In order to make the polished surfaces intimately contacted during fusion, polished fiber is intentionally fixed with slightly curved. The silicon substrate is then taken away by chemicals and such two samples are then assembled to be in contact status, transversely and longitudinally. This fiber assembly is then loaded onto the stage of our home-made arc fusion station shown in Fig. 2.6, equipped with a CCD camera. In our fusion station, the discharging electrodes are moved by a stepping motor and the intensity and duration of discharging can be programmed and adjusted.

The coupling condition is checked with ease by injecting a He-Ne laser light into a port of the contacted, polished fibers. The proximity of the two mated side-polished fibers is able to adjust by fine tuning the curvature of the fixed fibers through micrometers. We firstly start the discharging to clean contacted region with lower

temperature arc. Successively, the temperature is elevated to above 1500°C for fusion and the discharging arc is moving along the contacted, polished fibers, back and forth. Finally, the fused region is then proceeded to an annealing process, which leads to a good mechanical strength, with the same electrodes under a lower temperature. Here, fiber coupler with a fusion length of around 2.5 cm is accomplished. Insertion loss and mechanical strength are the major concerns of fiber couplers. In this work, the in-situ monitored red He-Ne laser light reveals the evolutions of coupling status and losses of our couplers. When fusing along the contacted interaction region of our coupler, the cross-coupling power changes periodically. No scattering loss is seen from a side-view shown in Fig. 2.7(a). The mechanical strength of the fused-polished region is excellent because of the thorough fusion between the two aligned polished fibers and the cross sectional views from coupler waist to coupler boundary are shown in Fig. 2.7(b). The two cores can be clearly observed but are somewhat deformed since the discharging power can not be well-controlled at this stage. This can be improved by designing electric circuits capable of operating in high-voltage and high-speed situations. An ASE white-light from EDFA is launched into the coupler and the wavelength separation spectrum which is obtained from the difference between the two output ports is shown in Fig. 2.8. The channel spacing is about 44 nm (1521 ~ 1565 nm). Finally, these fused-polished couplers are also tested well under various mechanical perturbations.

To the best of our knowledge, this is the first time for fused-polished fiber couplers to be fabricated through such an arc fusion. In contrast to those prior arts, the advantages are as follows. First, the intense and highly localized energy with temperature higher than 1500°C can be easily reached. This leads to a symmetrical cross-section and strong strength, which is helpful to good optical properties and Bragg grating formation on such kind of coupler, respectively. Second, a long effective interaction length is easily achieved which is useful to realize narrow-band fiber couplers, potentially. Furthermore, merits include easy control and potentially a low cost.

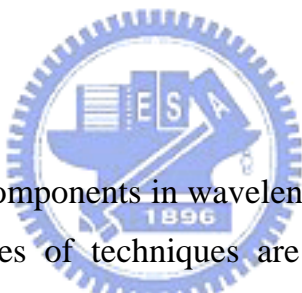
We have demonstrated preliminary fused-polished fiber couplers with a new fabrication method which shows promising in developing high-performance all-fiber

components like add/drop and CWDM multiplexers. Measurements on polarization dependence, adjustable coupling ratio at 1.55- μm band and a novel package are now in progress.

2.4 Narrowband Grating-Assisted Channel-Dropping Filter

Side-polished fiber couplers can serve as wavelength division multiplexers (WDM) with the channel spacing of around a few tens of nano-meters. However, to meet the requirements of dense wavelength division multiplexing (DWDM) systems, in which the typical channel spacing is of below one nano-meter, a fiber Bragg grating is useful to make side-polished fiber components as narrowband devices. In this section, I will demonstrate a narrowband channel-dropping filter using fiber Bragg gratings.

2.4.1 Introduction



Fiber add-drop filters are key components in wavelength division multiplexing (WDM) systems. In general, three types of techniques are used for fabrication, including micro-optics, phased-array waveguides [58], and fiber Bragg gratings. The idea of micro-optics filters is straightforward, but the manufacture of the whole assembly is labor-intensive: a multi-layered dielectric thin-film filter is sandwiched among fibers where each of their ends is butt-jointed with a grin lens for collimation. The commercial micro-optic filters are useful only for few-port applications because of the large insertion loss of approximately 0.7-0.9 dB for each wavelength dropped at its corresponding port. The phased-array waveguides are attractive for multi-port applications, but the associated techniques are too sophisticated and expensive [59]. In contrast, fiber Bragg gratings exhibit the narrowest bandwidth and provide the preferred all-fiber solution [60] such that we can directly couple the desired signals out of or into the transmission fibers with very low insertion loss.

By introducing UV-induced intra-core Bragg grating into the coupling section of either a fused-tapered coupler or of a side-polished coupler, all-fiber add-drop filters

were proposed and demonstrated [60]. Although directly fabricating a fiber Bragg grating into the elongated waist of a fused-tapered coupler looks elegant and causes a low insertion loss of around 0.1 dB [61], the dropping efficiency, spectral bandwidth and channel isolation for the dropped signal cannot be easily optimized simultaneously. This is due to the multi-mode excitation with the tapered transition of the fuse-tapered coupler which is a device based on cladding-mode coupling [62]. For such tapered devices, theoretical analyses have been carried out and found that even a small tilted angle of the inscribed grating can significantly downgrade the filtered signals [63]. The above modal conversion problem can be avoided by using the side-polished fiber coupler in which the cores are not deformed to excite higher-order modes. The coupling power is transferred through evanescent coupling and the coupling ratio is adjustable by controlling the coupling length. A 2×2 side-polished coupler containing intracore fiber Bragg grating(s) was proposed and demonstrated for add-drop filtering, however, the reflective spectra of the dropped signals were seriously broadened owing to the small radius of curvature of the polished fibers [17,64] and which can lead to a short coupling length. This is disadvantageous for a high-reflectivity narrow-band Bragg grating to be entirely enclosed at the coupling section. Accordingly, Baumann *et al.* increased the coupling length three times to 10 mm, but a very high insertion loss was reported in their work [64]. In addition, all studies relating to the side-polished fiber coupler showed well the unsolved difficulty in aligning two side-polished fibers.

By using silicon substrates and a home-made polisher, we achieved side-polished fibers with both a long interaction length and negligible losses [65,52]. In this work, we experimentally demonstrate the narrow-band channel-dropping filter using side-polished fibers with a long interaction length and an intra-core Bragg grating. Moreover, the alignment design is added onto silicon wafers using straight precision V-grooves alongside the polished fibers. Our study offers a promising fabrication method for high performance narrow-band add-drop multiplexers.

For a $1.55 \mu\text{m}$ single-mode side-polished fiber coupler, the incident light can excite the even and the odd modes in the interaction section of the couplers. The splitting-power ratios of the output signals depend on the phase difference between the two excited modes [66]. If a Bragg grating is introduced into one side of the

interaction section of a side-polished coupler as schematically shown in Fig. 2.9, the guiding wavelength matching the Bragg condition, namely the Bragg wavelength, can be reflected and then extracted from the drop port [64]. In addition, the extreme coupling power can be achieved by longitudinally offsetting the relative positions between two polished coupler-halves. For distinction, the side-polished fiber with a grating is called the grating coupler-half, and the side-polished fiber without grating is called the coupler-half. During fabrication, the side-polished fibers are embedded in curved V-grooves of a substrate and then polished. Their coupling strength is not uniform over the whole interaction region; thus we have to define an effective interaction length, L_{eff} [65]. In Fig. 2.9, the L_{eff} of a channel-dropping filter is composed of L_1 , L_g , and L_2 and is approximately proportional to the square root of the curvature radius [65]. A highly curved side-polished fiber not only leads to a short L_{eff} which cannot enclose a high-reflectivity narrow-band Bragg grating but also results in chirping of the grating period. These drawbacks degrade the reflectivity of the Bragg wavelength and also destroy the merits of the narrow-band nature of the Bragg grating. For the requirements of the dense wavelength division multiplexing (DWDM) systems, the length of a fiber grating with large reflectivity and narrow bandwidth is usually around 10 mm or more. Consequently, side-polished fibers with a larger radius of curvature are advantageous for performing narrow-band channel-dropping filters.

2.4.2 Experimental Results and Discussion

In our experiment, we used 1.55 μm single-mode photosensitive fibers with a numerical aperture of 0.13. The intra-core Bragg gratings were photoinduced into the fibers with a length of around 10 mm ($L_g = 10$ mm). As shown in Fig. 2.10, the stop-band bandwidth is 0.67 nm (3 dB) and the reflectivity is approximately 98.5%. A side lobe adjacent to the Bragg wavelength occurs due to the reuse of a fiber with a failed exposure prior time. These imperfections result from the fact that the UV exposure process by Industrial Technology Research Institute. Strictly speaking, the performance of the grating cannot satisfy well the general requirement for DWDM filters, i.e., the 99.9% reflectivity and a flat-top spectrum. Nevertheless, this study is

devoted to the performance of the side-polished channel-dropping filter with narrow bandwidth and high dropping efficiency ascribing to the long coupling length.

In the side-polishing process, we chose silicon wafers as our polishing substrates because of their advantages, as reported in our previous studies [65,52]. The accurate and rapid alignment can be achieved using the precision-etched silicon V-grooves. Consequently, two kinds of V-grooves are fabricated on the silicon substrates. The first set for fibers to be polished was a groove gradually widened from the center with a 1,200 cm curvature radius. The other set for aligning two side-polished fibers was a straight V-groove. In our fabrication processes, we employed a homemade polisher for polishing the exposed cladding away and the thickness of the exposed cladding was accurate because of the precision dimension of the V-groove. The surface of the silicon substrate can serve as the stop-monitor in polishing because its hardness is better than that of silica. This saves much time for side-polishing. The relative calibrations were presented in our previous studies [65,52]. Subsequently, well-polished fibers were cut into pieces where each piece has one fiber and two straight alignment V-grooves. Six well-polished fibers can be simultaneously fabricated within 20 min by us. To measure the spectra of the filtered signal, a C-band Amplified-Spontaneous-Emission (ASE) from an erbium-doped fiber amplifier is used as our light source and the signals are measured by an Ando optical spectrum analyzer of Model AQ6317B.

For comparison, we fabricated and measured more than 20 side-polished fiber gratings and found that their characteristics, before and after side-polishing. From these, we found their characteristics almost remained unchanged except for a small wavelength shift [67]. Fig. 2.10 shows the transmission spectrum of one of our grating coupler-halves in air. Because the Bragg wavelengths of these fiber gratings are not identical and their differences are much larger than their individual stopband bandwidth, we only consider asymmetric couplers here. The assembly and measurements for a channel-dropping filter are described as follows. Dummy fibers were embedded in the two alignment V-grooves of the first piece of the 5-cm-long sliced polished sample while their half depth was exactly beneath the silicon surface. The other polished sample was attached to the first one in the vertical position to form a coupler while the upper half of the dummy fibers went into its corresponding

alignment V-grooves. These dummy fibers can automatically achieve accurate alignment in the transverse direction of the coupler. This makes the phase-matching condition of the Bragg wavelength between the two polished fibers easily fulfilled. To facilitate our longitudinal alignment process and measurements, we used a 1×3 mechanical optical switch to monitor the drop port and the two transmission ports. By longitudinally adjusting the relative positions between the mated coupler-halves, we can achieve the best power coupling of the dropped signals from the drop port in a few minutes. For the perfect combination of the polished surfaces, their contact regions between two polished fibers should all be flat. Our side-polished samples are quite flat [65], but this flatness is maintained within a distance of a few millimeters. The length of our sliced wafer is much longer than the above value. Because of the present engineering drawback, we still require the adding of an index-matching liquid between the mated samples.

The measured characteristics of all our channel-dropping filters were all similar, and their insertion losses were less than 0.1 dB. Fig. 2.11 shows the spectra of (a) the drop port and (b) one transmission port (direct-through port) of one of our channel-dropping filters [68]. Note that the samples adopted for Figs. 2.10 and 2.11 were the same grating. In Fig. 2.9, the ASE was launched into the fiber from the input port. The measured dropping efficiency of the demonstrated channel-dropping filter, defined as the ratio of the dropped-wavelength power to Bragg-wavelength power from a grating coupler-half in air, is greater than 98%. All our well-polished samples can attain such a high efficiency. This clearly shows the advantages of the evanescent coupling over the cladding-mode coupling [60,61].

Successively, we examined the filtered bandwidth and found that the Bragg wavelength in Fig. 2.11 is slightly downshifted around 0.1 nm from that in Fig. 2.10. This wavelength shift is due to the variation of the effective mode index of the fiber grating derived from the use of the low-index-matching liquid between the polished surfaces [67]. Nevertheless, this effect has no influence on the performance of the narrow-band nature of the fiber Bragg gratings. A large effective coupling length dominates the narrow-band characteristics of the side-polished channel-dropping filters and therefore a large curvature radius of the polished fibers is important. Note

that in Fig. 2.11(a), the filtered bandwidth of the drop port is less than 2 nm (25 dB) which deviates less from that of the grating coupler-half in air.

Among all side-polished fiber channel-dropping filters published so far, the largest L_{eff} was equal to 10 mm, to the best of our knowledge [64]. However, the resulting bandwidth of 5 nm (25 dB) and an excessive insertion loss as large as 7 dB were measured. The alignment of the two polished fibers using precision micrometers was elaborate [64]. Consequently, our study offers a promising fabrication method for high-performance devices in various applications. Finally, the temperature dependence of Bragg grating [60] is an issue for side-polished channel-dropping filters in DWDM system applications. Fiber gratings should be packaged with a kind of thermal expansion compensation and is very difficult for us to achieve at present.

In conjunction with side-polished fibers and intra-core fiber Bragg gratings, we demonstrate fiber channel-dropping filters with the spectral bandwidth (25 dB) less than 2 nm, a dropping efficiency greater than 98% from the 98.5% reflectivity of the grating and channel isolation greater than 25 dB. During fabrication, fibers are embedded in a silicon wafer and simultaneously polished. Alignment V-grooves are fabricated on our silicon substrate to greatly facilitate the alignment work. This fabrication method is fast and reliable. However, to ensure a long and flat contact between two mated surfaces, adding an index-matching liquid between the polished surfaces is currently necessary and this will be improved soon. Narrow-band all-fiber add/drop multiplexers could also be realized on the basis of our long polished fibers if two identical fiber gratings are both introduced at the coupling region [64].

References

- [1] R. A. Bergh, H. C. Lefevre, and H. J. Shaw, "All-single-mode fiber-optic gyroscope," *Opt. Lett.* **6**, 198-200 (1981).
- [2] R. A. Bergh, G. Kotler, and H. J. Shaw, "Single-mode fiber optics directional coupler," *Electron. Lett.* **16**, 260-261 (1980).
- [3] M. J. F. Digonnet and H. J. Shaw, "Analysis of a tunable single mode optical fiber coupler," *IEEE J. Quantum Electron.* **QE-18**, 746-754 (1982).
- [4] M. Digonnet and H. J. Shaw, "Wavelength multiplexing in single-mode fiber

- couplers,” *Appl. Opt.* **22**, 484-491 (1983).
- [5] O. Parriaux, S. Gidon, and A. A. Kuznetsov, “Distributed coupling on polished single-mode optical fibers,” *Appl. Opt.* **20**, 2420-2423 (1981).
- [6] A. W. Snyder and A. J. Stevenson, “Polished-type couplers acting as polarizing beam splitters,” *Opt. Lett.* **11**, 254-256 (1986).
- [7] K. Thyagarajan, S. Diggavi, and A. K. Ghatak, “Design and analysis of a novel polarization splitting directional coupler,” *Electron. Lett.* **24**, 869-870 (1988).
- [8] J. E. Bowers, S. A. Newton, and H. J. Shaw, “Fibre-optic variable delay lines,” *Electron. Lett.* **18**, 999-1000 (1982).
- [9] S. A. Newton, K. P. Jackson, and H. J. Shaw, “Optical fiber V-groove transversal filter,” *Appl. Phys. Lett.* **43**, 149-151 (1983).
- [10] J. V. Wright, S. R. Mallinson, and C. A. Millar, “A fiber-based crosspoint switch using high refractive index interlay materials,” *IEEE J. Sel. Commun.* **6**, 1160-1168 (1988).
- [11] K. McCallion, W. Johnstone, and G. Thursby, “Investigation of optical fibre switch using electro-optic interlays,” *Electron. Lett.* **28**, 410-411 (1992).
- [12] S. M. Tseng and C. L. Chen, “Low-voltage optical fiber switch,” *Jpn J. Appl. Phys.* **37**, L42-L45 (1998).
- [13] W. V. Sorin, P. Zorabedian, and S. A. Newton, “Tunable single-mode fiber reflective grating filter,” *J. Lightwave Technol.* **LT-5**, 1199-1202 (1987).
- [14] R. B. Charters, A. P. Kuczynski, S. E. Satines, R. P. Tatam, and G. J. Ashwell, “In-line fibre optic channel dropping filter using Langmuir-Blodgett films,” *Electron. Lett.* **30**, 594-595 (1994).
- [15] W. Johnstone, G. Thursby, D. Moodie, R. Varshney, and B. Culshaw, “Fibre optic wavelength channel selector with high resolution,” *Electron. Lett.* **28**, 1364-1365 (1992).
- [16] D. G. Moodie, and W. Johnstone, “Wavelength tenability of components based on the evanescent coupling from a side-polished fiber to a high-index-overlay waveguide,” *Opt. Lett.* **18**, 1025-1027 (1993).
- [17] J. L. Archambault, P. St. J. Russell, S. Barchlos, P. Hua, and L. Reekie, “Grating-frustrated coupler: a novel channel-dropping filter in single-mode

- optical fiber,” *Opt. Lett.* **19**, 180-182 (1994).
- [18] K. R. Sohn and J. W. Song, “Thermooptically tunable side-polished fiber comb filter and its application,” *IEEE Photon. Technol. Lett.* **14**, 1575-1577 (2002).
- [19] K. T. Kim, S. Hwang-bo, G. I. Kweon, and S. R. Choi, “Widely tunable filter based on side-polished polarization-maintaining fibre coupled with thermo-optic polymer overlay,” *Electron. Lett.* **40**, 1330-1332 (2004).
- [20] J. R. Feth and C. L. Chang, “Metal-clad fiber-optic cutoff polarizer,” *Opt. Lett.* **11**, 386-388 (1986).
- [21] S. G. Lee, J. P. Sokoloff, B. P. McGinnis, and H. Sasabe, “Fabrication of a side-polished fiber polarizer with a birefringent polymer overlay,” *Opt. Lett.* **22**, 606-608 (1997).
- [22] T. Hosaka, K. Okamoto, and T. Edahiro, “Fiber circular polarizer,” *Appl. Opt.* **22**, 3850-3858 (1983).
- [23] S. P. Ma and S. M. Tseng, “High-performance side-polished fibers and applications as liquid crystal clad fiber polarizers,” *IEEE Photon. Technol. Lett.* **15**, 1554-1556 (1997).
- [24] Z. K. Ioannidis, I. P. Giles, and C. Bowry, “All-fiber optic intensity modulators using liquid crystals,” *Appl. Opt.* **30**, 328-333 (1991).
- [25] G. Fawcett, W. Johnstone, I. Andonovic, D. J. Bone, T. G. Harvey, N. Carter, and T. G. Ryan, “In-line fibre-optic intensity modulator using electro-optic polymer,” *Electron. Lett.* **28**, 985-986 (1992).
- [26] M. Wilkinson, J. R. Hill, and S. A. Cassidy, “Optical fibre modulator using electro-optic polymer overlay,” *Electron. Lett.* **27**, 980-981 (1991).
- [27] O. I. Baum, N. V. Varlamova, B. I. Zapadinskii, G. V. Mishakov, and V. I. Sokolov, “Continuously tunable fibre attenuator operating in the wavelength range near 1.5 μm ,” *Quantum Electron.* **34**, 849-851 (2004).
- [28] G. Raizada and B. P. Pal, “Refractometers and tunable components based on side-polished fibers with multimode overlay waveguides: role of the superstrate,” *Opt. Lett.* **21**, 399-401 (1996).
- [29] W. Johnstone, G. Thursby, D. Moodie, and K. McCallion, “Fiber-optic refractometer that utilizes multimode waveguide overlay devices,” *Opt. Lett.* **17**,

- 1538-1540 (1992).
- [30] N. Periasamy and F. P. Schäfer, "Laser amplification in an optical fiber by evanescent field coupling," *Appl. Phys.* **24**, 201-203 (1981).
- [31] W. V. Sorin, K. P. Jackson, and H. J. Shaw, "Evanescent amplification in a single-mode optical fibre," *Electron. Lett.* **19**, 820-821 (1983).
- [32] V. A. Kozlov, V. V. Ter-Mikirtychev, and T. Tsuboi, "In-line singlemode fibre amplifiers based on LiF:F_2^+ and LiF:F_2^- crystals," *Electron. Lett.* **31**, 2104-2105 (1995).
- [33] C. W. Lee, K. Kim, J. Noh, and W. Jhe, "Quantum theory of amplified total internal reflection due to evanescent-mode coupling," *Phys. Rev. A.* **62**, Art. No. 053805 (2000).
- [34] W. Hodel, P. Anliker, and H. P. Weber, "Analysis of a single-mode evanescent-field-pumped dye amplifier," *J. Lightwave Technol.* **LT-1**, 470-475 (1983).
- [35] W. V. Sorin and M. H. Yu, "Single-mode-fiber ring dye-laser," *Opt. Lett.* **10**, 550-552 (1985).
- [36] W. G. Jung, S. W. Kim, K. T. Kim, E. S. Kim, and S. W. Kang, "High-sensitivity temperature sensor using a side-polished single-mode fiber covered with the polymer planar waveguide," *IEEE Photon. Technol. Lett.* **13**, 1209-1211 (2001).
- [37] H. Tai, H. Tanaka, and T. Yoshino, "Fiber-optic evanescent-wave methane-gas sensor using optical absorption for the 3.392- μm line of a He-Ne laser," *Opt. Lett.* **12**, 437-439 (1987).
- [38] A. Messica, A. Greenstein, A. Katzir, U. Schiessl, and M. Tacke, "Fiber-optic evanescent wave sensor for gas detection," *Opt. Lett.* **19**, 1167-1169 (1994).
- [39] A. Gaston, F. Perez, and J. Sevilla, "Optical fiber relative-humidity sensor with polyvinyl alcohol film," *Appl. Opt.* **43**, 4127-4132 (2004).
- [40] A. Gaston, I. Lozano, F. Perez, F. Auza, and J. Sevilla, "Evanescent wave optical-fiber sensing (temperature, relative humidity, and pH sensors)," *IEEE Sensors Journal* **3**, 806-811 (2003).
- [41] A. Alvarez-Herrero, H. Guerrero, T. Berenguer, and D. Levy, "High-sensitivity

- temperature sensor base don overlay on side-polished fibers,” IEEE Photon. Technol. Lett. **12**, 1043-1045 (2000).
- [42] D. C. Bownass, J. S. Barton, and J. D. C. Jones, “Serially multiplexed point sensor for the detection of high humidity in passive optical networks,” Opt. Lett. **22**, 346-348 (1997).
- [43] C. D. Hussey and J. D. Minelly, “Optical fibre polishing with a motor-driven polishing wheel,” Electron. Lett. **24**, 805-807 (1988).
- [44] R. P. Dahlgren and N. H. Katis, “Computer-controlled technique for cutting curved grooves in polished fiber-optic coupler substrates,” IEEE Photon. Technol. Lett. **5**, 1227-1230 (1993).
- [45] A. K. Das, M. A. Mondal, A. Mukherjee, and A. K. Mandal, “Automatic determination of the remaining cladding thickness of a single-mode fiber half-coupler,” Opt. Lett. **19**, 384-386 (1994).
- [46] M. J. F. Digonnet, J. R. Feth, L. F. Stokes, and H. J. Shaw, “Measurement of the core proximity in polished fiber substrates and couplers,” Opt. Lett. **10**, 463-465 (1985).
- [47] R. P. Severin, “Multipurpose single-mode fibre-optic coupling substrate, made with silicon etch and polish technique,” Electron. Lett. **25**, 969-970 (1989).
- [48] S. M. Tseng and C. L. Chen, “Side-polished fibers,” Appl. Opt. **31**, 3438-3447 (1992).
- [49] N. K. Chen, S. Chi, and S. M. Tseng, “Narrow-band channel-dropping filter based on side-polished fiber with long interaction length,” Jpn. J. Appl. Phys. **43**, L475-L477 (2004).
- [50] N. K. Chen and S. Chi, “Evanescent wave photonic crystal fiber tunable filter using dispersive polymers,” in Proceeding of Optical Fiber Communication Conference (OFC 2005), Anaheim, USA, Mar. 6-11, 2005. OWD3.
- [51] N. K. Chen, S. Chi, L. Zhang, L. Hu, K. P. Chuang, Y. Lai, S. M. Tseng, and J. T. Shy, “CW-pumped evanescent amplification at 1.55 μm wavelength using highly Er^{3+} -doped glass over side-polished fiber,” CLEO 2005 conference, Baltimore, USA, May 22-27, 2005. JWB61.
- [52] S. P. Ma and S. M. Tseng, “High-performance side-polished fibers and

- applications as liquid crystal clad fiber polarizers,” *J. Lightwave Technol.* **15**, 1554-1558 (1997).
- [53] B. S. Kawasaki, and K. O. Hill, “Low-loss access coupler for multimode optical fiber distribution networks,” *Electron. Lett.* **16**, 1794-1795 (1977).
- [54] E. Marin, R. Ghosh, J.-P. Meunier, X. Daxhelet, and S. Lacroix, “Bragg gratings in 2×2 symmetric fused fiber couplers: influence of the tilt on the wavelength response,” *IEEE Photonics Technol. Lett.*, **11**, 1434-1436 (1999).
- [55] R. A. Burgh, G. Kotler, and H. J. Shaw, “Single-mode fibre optic directional coupler,” *Electron. Lett.* **16**, 260-261 (1980).
- [56] C. V. Cryan, and C. D. Hussey, “Fused polished single mode fibre couplers,” *Electron. Lett.* **28**, 204-205 (1992).
- [57] N. K. Chen, S. Chi, and S. M. Tseng, “Evanescent-field fiber combiners for 1310/1550-nm and 1480/1550-nm wavelengths,” *Proceedings of Optics and Photonics Taiwan’02*, **2**, 497-499 (2002).
- [58] E. Pennings, G. D. Khoe, M. K. Smit, and T. Staring, “Integrated-optic versus microoptic devices for fiber-optic telecommunication systems: a comparison,” *IEEE J. Sel. Topics Quantum Electron.* **2**, 151-164 (1996).
- [59] N. Ofusa, T. Saito, T. Shimoda, T. Hanada, Y. Urino, and M. Kitamura, “An optical add-drop multiplexer with a grating-loaded directional coupler in silica waveguides,” *IEICE Trans. Commun.* **E82-B**, 1248-1251 (1999).
- [60] A. Othonos and K. Kalli, *Fiber Bragg Gratings*, (Artech House, Boston, 1999).
- [61] A. S. Kewitsch, G. A. Rakuljic, P. A. Willems and A. Yariv, “All-fiber zero-insertion-loss add-drop filter for wavelength-division multiplexing,” *Opt. Lett.* **23**, 106-108 (1998).
- [62] T. A. Birks and Y. W. Li, “The shape of fiber tapers,” *IEEE J. Lightwave Technol.* **10**, 432-438 (1992).
- [63] E. Marin, R. Ghosh, J.-P. Meunier, X. Daxhelet, and S. Lacroix, “Bragg gratings in 2×2 symmetric fused fiber couplers: Influence of the tilt on the wavelength response,” *IEEE Photon. Technol. Lett.* **11**, 1434-1436 (1999).
- [64] I. Baumann, J. Seifert, W. Nowak, and M. Sauer, “Compact all-fiber add-drop-multiplexer using fiber Bragg gratings,” *IEEE Photon. Technol. Lett.* **8**,

1331-1333 (1996).

- [65] K. Y. Hsu, S. P. Ma, K. F. Chen, S. M. Tseng, and J. I. Chen, "Surface-polariton fiber polarizer: Design and experiment," *Jpn. J. Appl. Phys.* **36**, L488-L490 (1997).
- [66] A. W. Snyder and J. D. Love: *Optical Waveguide Theory* (Chapman and Hall, New York, 1983).
- [67] S. M. Tseng, S. P. Ma, K. Y. Hsu, K. Tai, and Y. Lai, "Tunable optical filter or reflector," U.S. Patent 5809188 (1998).
- [68] N. K. Chen, S. Chi, and S. M. Tseng, "Low-Loss Fiber De-Multiplexers," *Proc. OECC'03*, Shanghai, 2003 (Science Press, Beijing, 2003) p. 127-128.



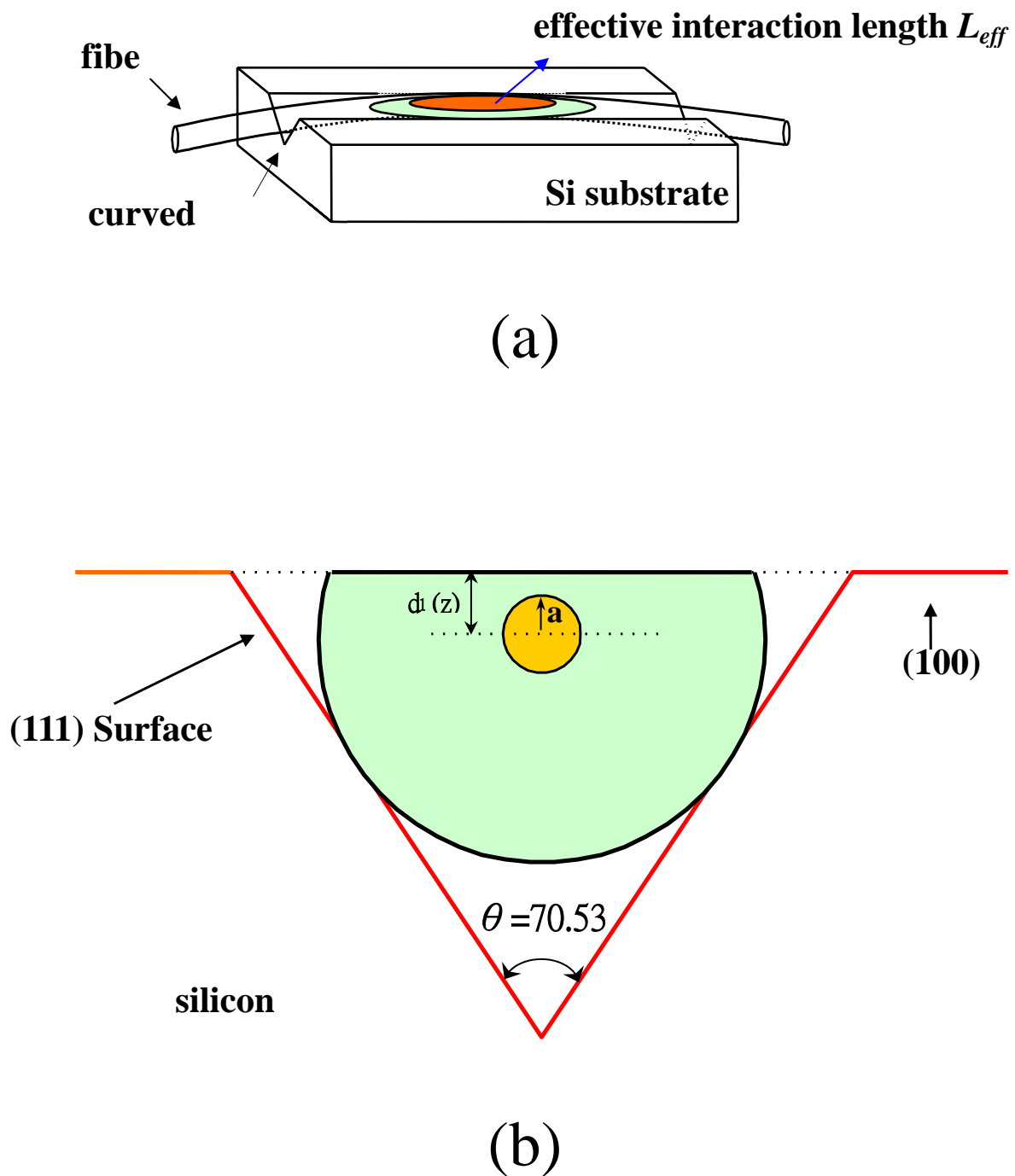
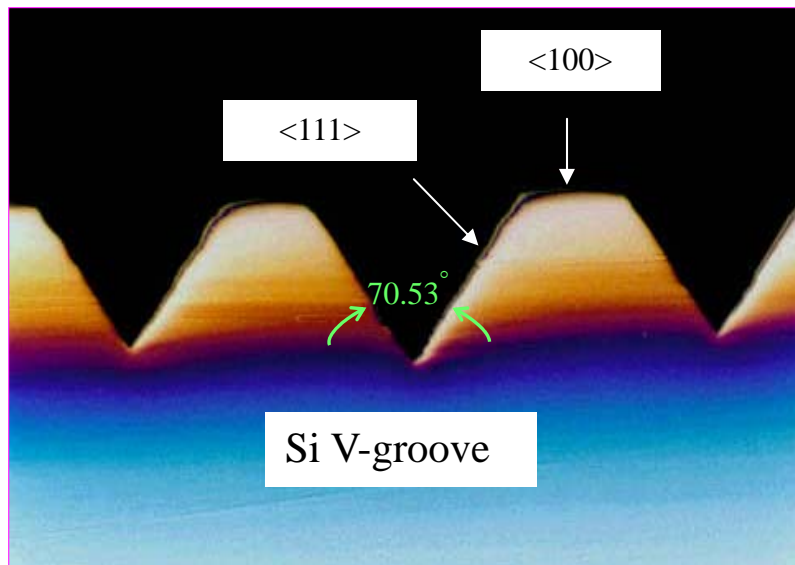
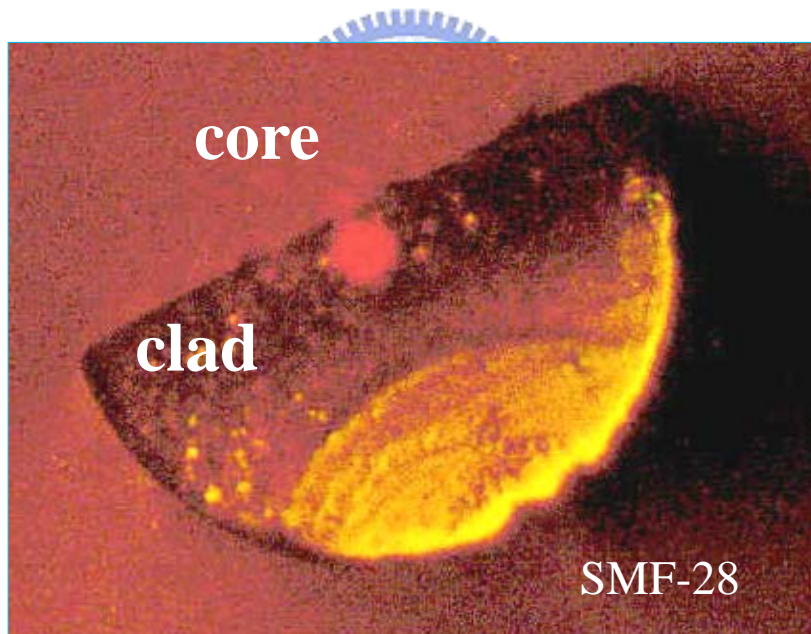


Fig. 2.1 Schematics of the (a) side-view of the side-polished fiber and (b) cross sectional view of the side-polished fiber in the V-groove.

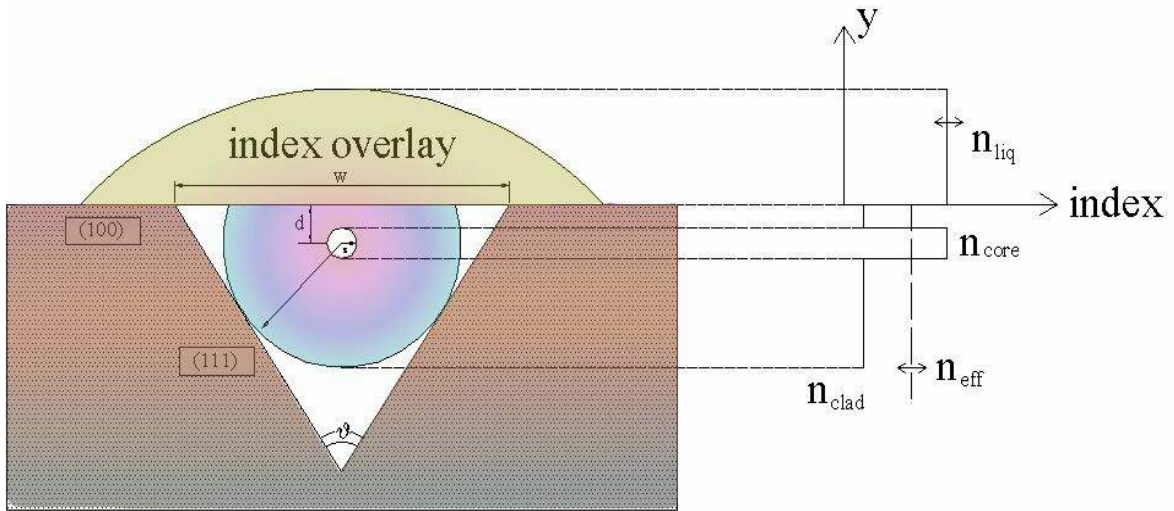


(a)

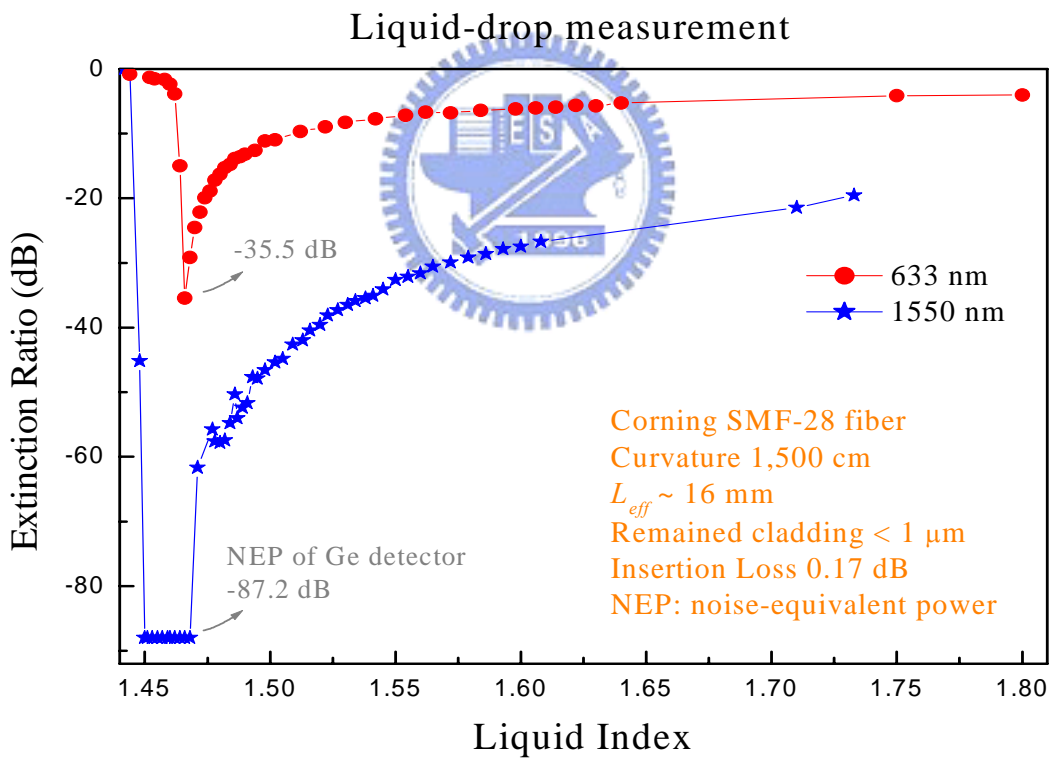


(b)

Fig. 2.2 (a) Silicon V-grooves. Central V-groove is for side-polished fiber while adjacent two V-grooves are for alignment fibers. (b) Cross sectional view of the side-polished single-mode fiber. A He-Ne laser light is launched into the core.



(a)



(b)

Fig. 2.3 Wavelength tunability of the short-pass filter using SP-SMF-28 with OCK-433 overlay through thermo-tuning. Resolution: 1 nm. R : 15 m.

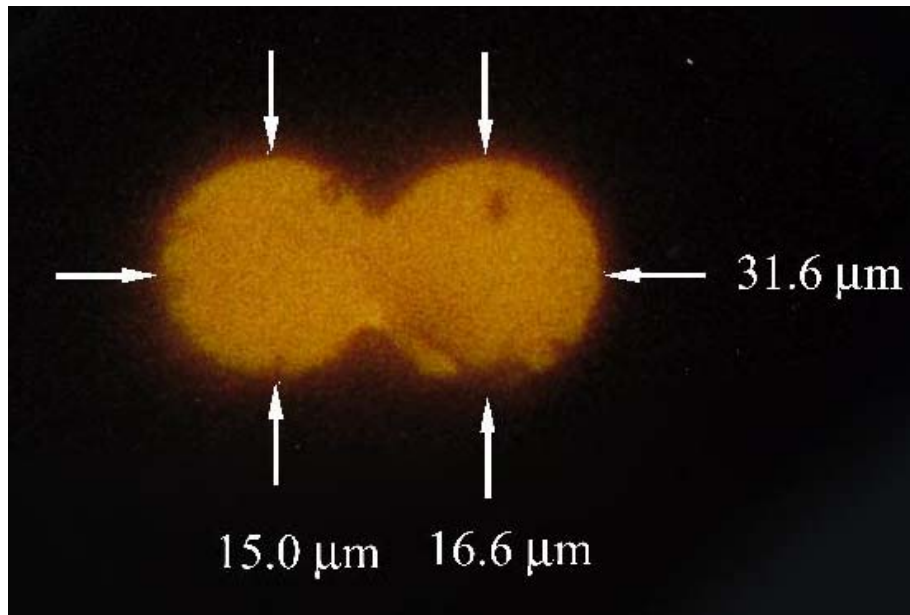


Fig. 2.4 Cross sectional view of the fused-tapered fiber coupler. The guiding area is in a dumbbell shape to degrade the polarization isotropy.

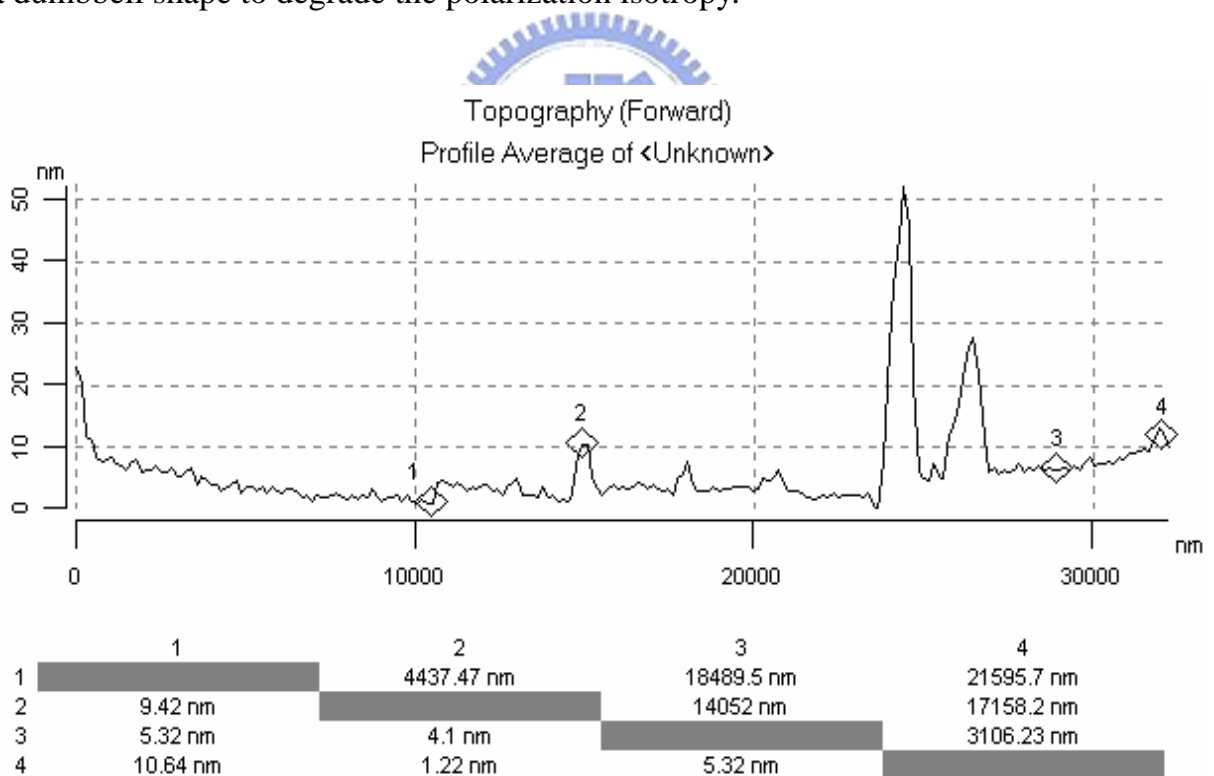


Fig. 2.5 Surface roughness of the side-polished fiber measured by AFM. The major two peaks are due to dust.

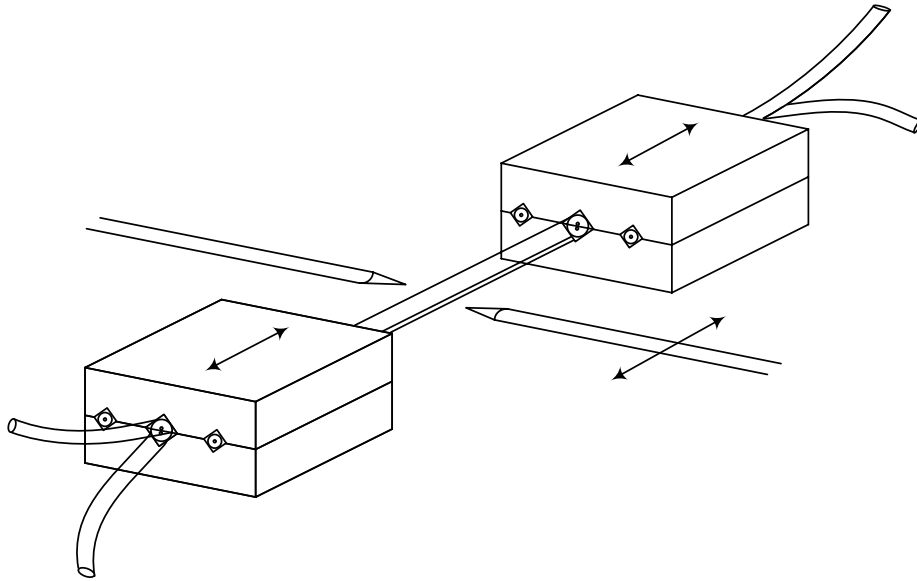
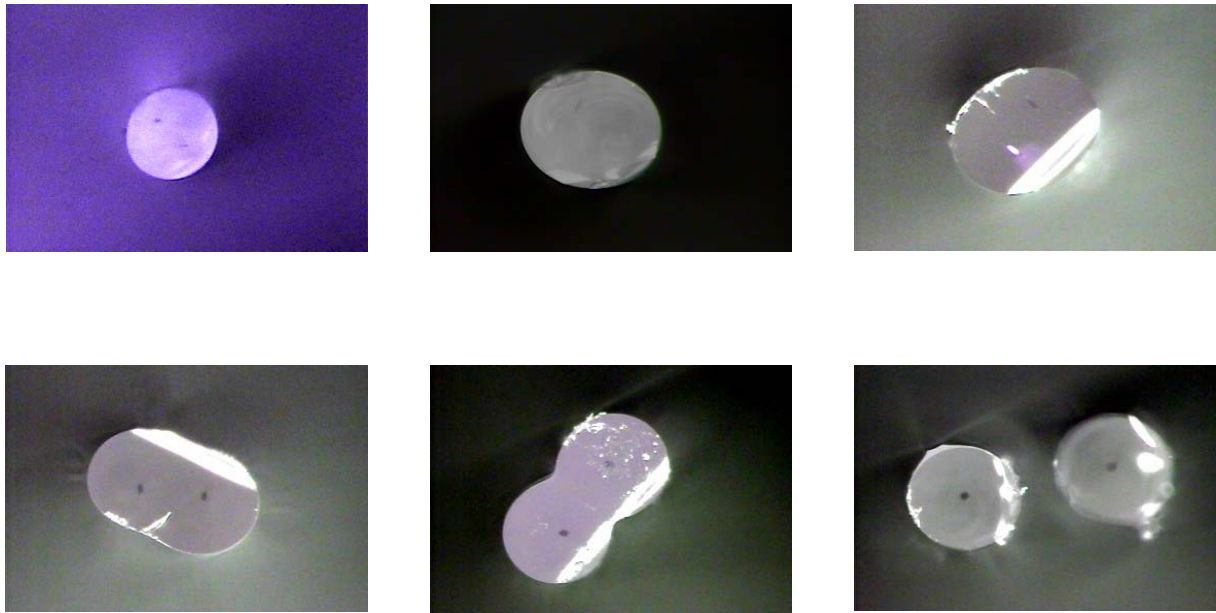


Fig. 2.6 Schematic of the fabrication of a fused-polished fiber coupler using a moving arc. The sliding silicon V-grooves serve as alignment devices.



(a)



(b)

Fig. 2.7 (a) Side-view and (b) cross-sectional views of the fused-polished fiber coupler.

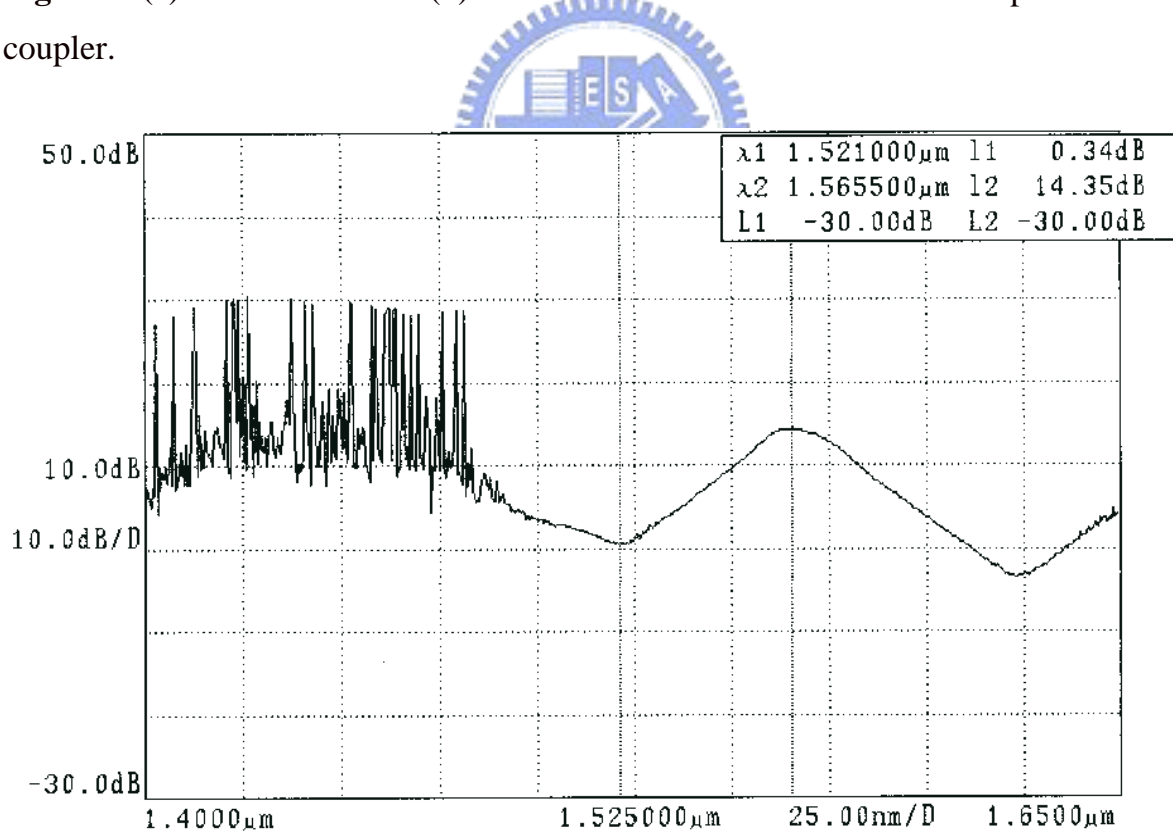


Fig. 2.8 Wavelength separation spectrum of the fused-polished coupler where the channel spacing is 44 nm (1521 ~ 1565 nm). The left part noise is due to the weak power level of the C+L band ASE light source below 1500 nm wavelength region.

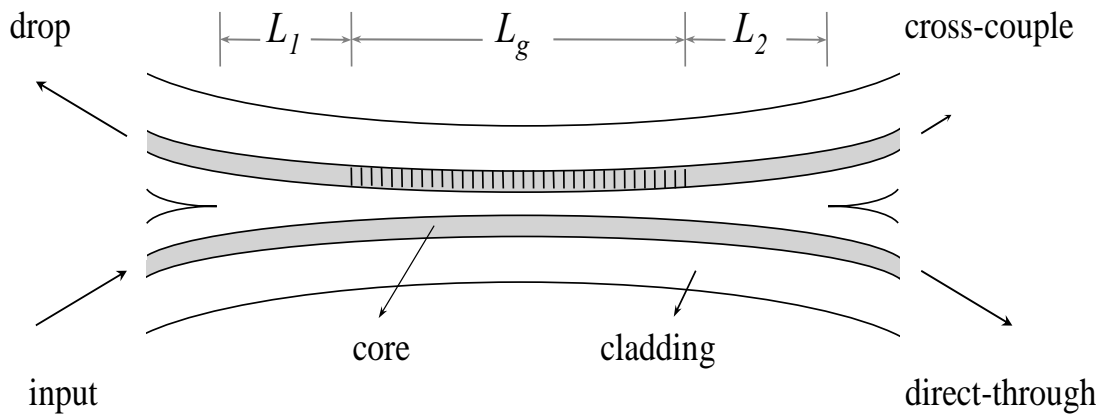


Fig. 2.9 Schematic diagram of our narrowband channel-dropping filter.

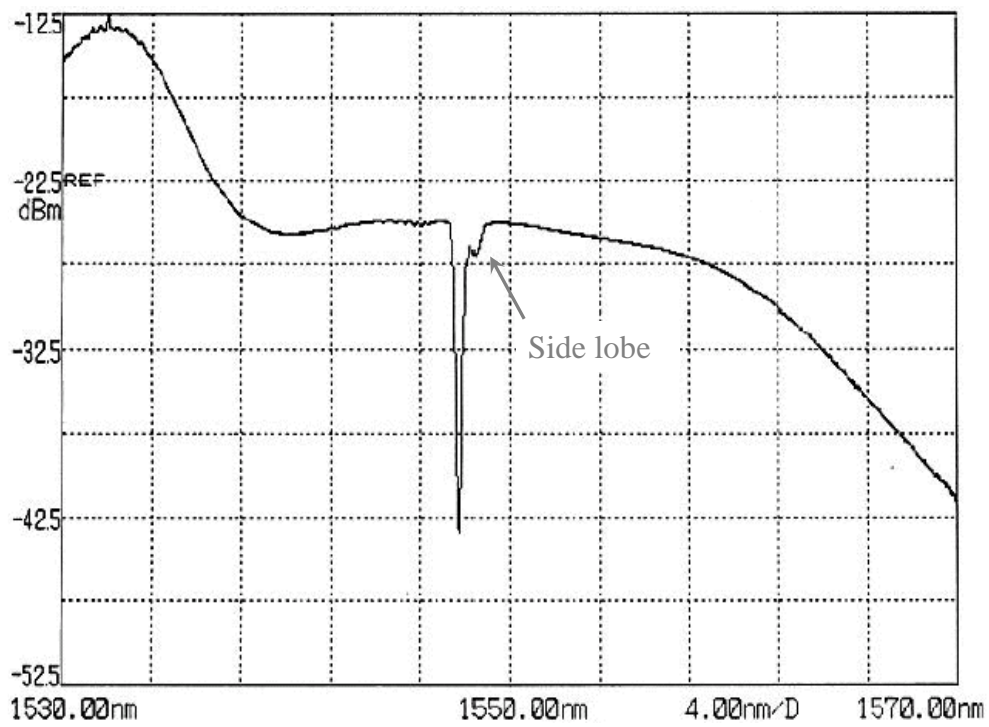


Fig. 2.10 Transmission spectrum of a grating coupler-half in air. The resolution is 0.1 nm.

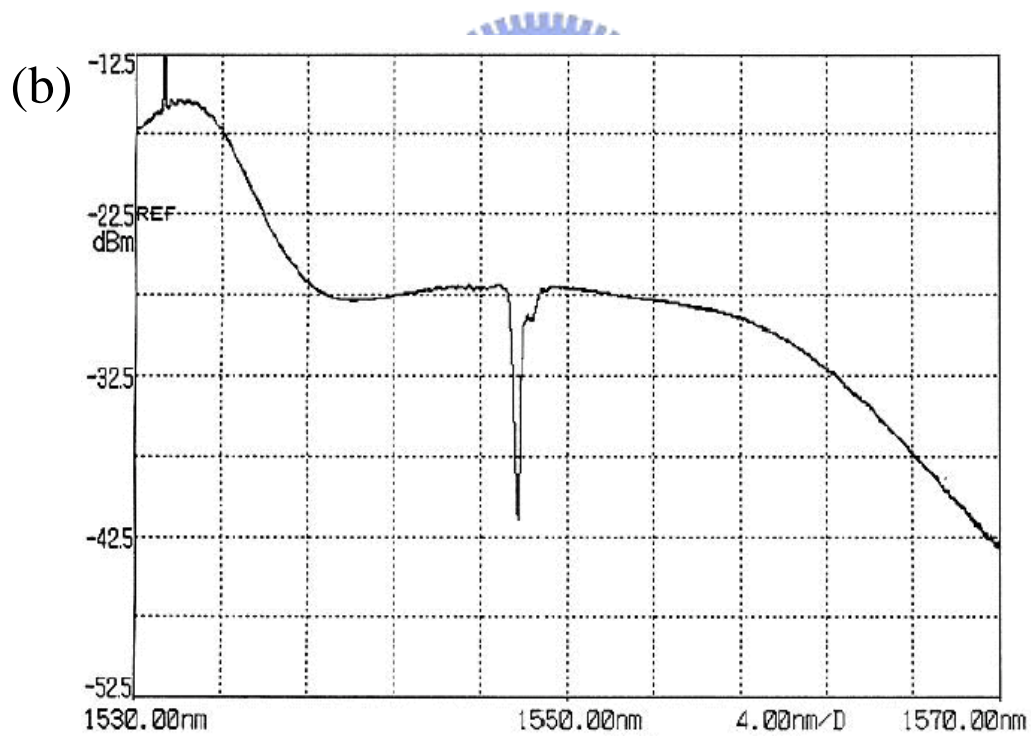
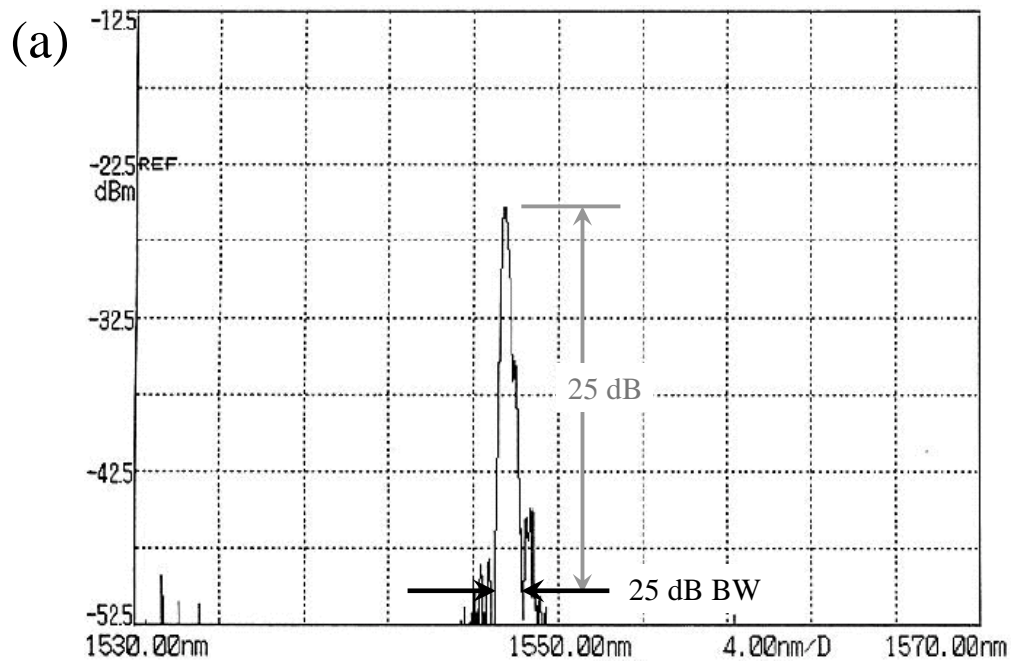


Fig. 2.11 Measured spectra from (a) drop port and (b) direct-through port of the assembled channel-dropping filter. The resolution is 0.1 nm.